

---

# Neural Analogical Matching

---

**Maxwell Crouse**  
Qualitative Reasoning Group  
Northwestern University  
mvcrouse@u.northwestern.edu

**Constantine Nakos**  
Qualitative Reasoning Group  
Northwestern University  
cnakos@u.northwestern.edu

**Ibrahim Abdelaziz**  
IBM Research  
IBM T.J. Watson Research Center  
ibrahim.abdelaziz1@ibm.com

**Kenneth Forbus**  
Qualitative Reasoning Group  
Northwestern University  
forbus@northwestern.edu

## Abstract

Analogy is core to human cognition. It allows us to solve problems based on prior experience, it governs the way we conceptualize new information, and it even influences our visual perception. The importance of analogy to humans has made it an active area of research in the broader field of artificial intelligence, resulting in data-efficient models that learn and reason in human-like ways. While analogy and deep learning have generally been studied independently of one another, the integration of the two lines of research seems like a promising step towards more robust and efficient learning techniques. As part of the first steps towards such an integration, we introduce the Analogical Matching Network: a neural architecture that learns to produce analogies between structured, symbolic representations that are largely consistent with the principles of Structure-Mapping Theory.

## 1 Introduction

Analogical reasoning is a form of inductive reasoning that cognitive scientists consider to be one of the cornerstones of human intelligence [1, 2, 3]. Analogy shows up at nearly every level of human cognition, from low-level visual processing [4] to abstract conceptual change [5]. Problem solving using analogy is common, with past solutions forming the basis for dealing with new problems [6, 7]. Analogy also facilitates learning and understanding by allowing people to generalize specific situations into increasingly abstract schemas [8].

Many different theories have been proposed for how humans perform analogy [9, 10, 11, 12]. One of the most influential theories is Structure-Mapping Theory (SMT) [11], which posits that analogy involves the alignment of structured representations of objects or situations subject to certain constraints. Key characteristics of SMT are its use of symbolic representations and its emphasis on relational structure, which allow the same principles to apply to a wide variety of domains.

Until now, the symbolic, structured nature of SMT has made it a poor fit for deep learning. The representations produced by deep learning techniques are incompatible with off-the-shelf SMT implementations like the Structure-Mapping Engine (SME) [13], while the symbolic graphs that SMT assumes as input are challenging to encode with traditional neural methods. However, recent advances in deep learning have made it possible to bridge the gap between the two traditions, providing the architectural tools needed to create neural networks that can learn to produce analogies.

**Contributions:** We introduce the Analogical Matching Network (AMN), a neural architecture that learns to produce analogies between symbolic representations. Though trained on purely synthetic data, we show over a diverse set of existing analogy problems that AMN’s outputs are largely

consistent with SMT. With AMN, we aim to push the boundaries of deep learning and extend them to an important area of human cognition. It is our hope that future generations of neural architectures can reap the same benefits from analogy that symbolic reasoning systems and humans currently do.

## 2 Related Work

Many different computational models of analogy have been proposed [14, 15, 13], each instantiating a different cognitive theory of analogy. The differences between them are compounded by the computational costs of analogical reasoning, a provably NP-HARD problem [16]. These computational models are often used to test cognitive theories of human behavior, but they are also useful tools for applied tasks. For instance, the computational model we compare AMN to in this work, the Structure-Mapping Engine (SME), has been used in natural language question-answering [17, 18], computer vision [19, 20], and machine reasoning [21, 22].

Many of the early approaches to analogy were connectionist [23]. The STAR architecture of [24] used tensor product representations of structured data to perform simple analogies of the form  $R(x, y) \Rightarrow S(f(x), f(y))$ . Drama [25] was an implementation of the multi-constraint theory of analogy [12] that employed a holographic representation similar to tensor products to embed structure. LISA [26, 27] was a hybrid symbolic connectionist approach to analogy. It staged the mapping process temporally, generating mappings from elements of the compared representations that were activated at the same time.

Cognitive perspectives of analogy have gone relatively unexplored in deep learning research, with only a few recent works that address them [28, 29]. Generally, prior deep learning work has only considered analogies of the form  $A : B :: C : D$  [30, 31], where the task would be to identify a relation that holds across a set of examples and then apply it to novel data. Still, such prior works demonstrated progress in applying analogy to more natural perceptual data in the form of images or language. As of yet, no work has explored a deep learning approach to analogy that operates over the graph-based symbolic representations used in standard computational models of analogy.

## 3 Structure-Mapping Theory

In Structure-Mapping Theory (SMT) [11], analogy centers around the structural alignment of *relational representations* (see Figure 1). A relational representation is a set of logical expressions constructed from entities (e.g., sun), attributes (e.g., YELLOW), functions (e.g., TEMPERATURE), and relations (e.g., GREATER). Structural alignment is the process of producing a *mapping* between two relational representations (referred to as the *base* and *target*). A mapping is a triple  $\langle M, C, S \rangle$ , where  $M$  is a set of *correspondences* between the base and target,  $C$  is a set of *candidate inferences* (i.e., inferences about the target that can be made from the structure of the base), and  $S$  is a *structural evaluation score* that measures the quality of  $M$ . Correspondences are pairs of elements between the base and target (i.e., expressions or entities) that are identified as matching with one another. While entities can be matched together irrespective of their labels, there are more rigorous criteria for matching expressions. SMT asserts that matches should satisfy the following properties:

1. *One-to-One*: Each element of the base and target can be a part of *at most* one correspondence.
2. *Parallel Connectivity*: Two expressions can be in a correspondence with each other only if their arguments are also in correspondences with each other.
3. *Tiered Identicality*: Relations of expressions in a correspondence must match identically, but functions need not be identical if their correspondence would support structural connectivity.
4. *Systematicity*: Preference should be given to mappings with more deeply nested expressions.

To understand these properties, we will use the example in Figure 1, which draws an analogy between the Solar System and the Rutherford model of the atom. A set of correspondences  $M$  between the base (Solar System) and target (Rutherford atom) is a set of pairs of elements from both sets, e.g.,  $\{\langle [1], [8] \rangle, \langle [2], [9] \rangle\}$ . The one-to-one constraint restricts each element to be a member of at most one correspondence. Thus, if  $\langle [7], [15] \rangle$  was a member of  $M$ , then  $\langle [7], [16] \rangle$  could not be added to  $M$ . Parallel connectivity enforces correspondence between arguments if the parents are in correspondence. In this example, if  $\langle [7], [15] \rangle$  was a member of  $M$ , then both  $\langle [3], [10] \rangle$  and

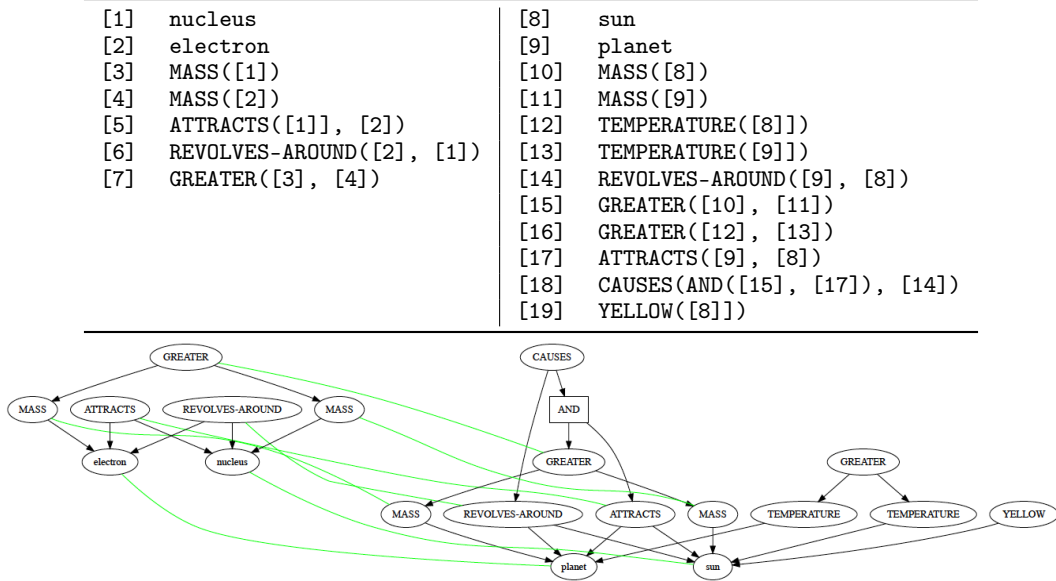


Figure 1: Relational and graph representations for models of the atom (left) and Solar System (right). Light green edges indicate the set of correspondences between the two graphs.

$\langle [4], [11] \rangle$  would need to be members of  $M$ . In addition, parallel connectivity respects argument order when dealing with ordered relations. Tiered identity is not relevant in this example; however, if [10] used the label WEIGHT instead of MASS, tiered identity could be used to match [3] and [10], since such a correspondence would allow for a match between their parents. The last property, systematicity, results in larger correspondence sets being preferred over smaller ones. Note that the singleton set  $\{\langle [1], [8] \rangle\}$  satisfies SMT’s constraints, but it is clearly not useful by itself. Systematicity captures the natural preference for larger, more interesting matches.

Candidate inferences are statements from the base that are projected into the target to fill in missing structure [23, 32, 33]. Given a set of correspondences  $M$ , candidate inferences are created from statements in the base that are supported by expressions in  $M$  but are not part of  $M$  themselves. Returning to Figure 1, one candidate inference would be  $\text{CAUSES}(\text{AND}([7], [5]), [6])$ , derived from [18] by substituting its arguments with the expressions they correspond to in the target. In this work, we adopt SME’s default criteria for computing candidate inferences. Valid candidate inferences are all statements that have *some* dependency that is included in the correspondences or an ancestor that is a candidate inference (e.g., an expression whose parent has arguments in the correspondences).

The concepts above carry over naturally into graph-theoretic notions. The base and target are considered semi-ordered directed-acyclic graphs (DAGs)  $G_B = \langle V_B, E_B \rangle$  and  $G_T = \langle V_T, E_T \rangle$ , where  $V_B$  and  $V_T$  are sets of nodes and  $E_B$  and  $E_T$  are sets of edges. Each node corresponds to some expression and has a label given by its relation, function, attribute, or entity name. Structural alignment is the process of finding a maximum weight bipartite matching  $M \subseteq V_B \times V_T$ , where  $M$  satisfies the pairwise-disjunctive constraints imposed by parallel connectivity. Finding candidate inferences is then determining the subset of nodes from  $V_B \setminus \{b_i : \langle b_i, t_j \rangle \in M\}$  with support in  $M$ .

## 4 Model

### 4.1 Model Components

Given a base  $G_B = \langle V_B, E_B \rangle$  and target  $G_T = \langle V_T, E_T \rangle$ , AMN produces a set of correspondences  $M \subseteq V_B \times V_T$  and a set of candidate inferences  $I \in V_B \setminus \{b_i : \langle b_i, t_j \rangle \in M\}$ . A key design choice of this work was to avoid using rules or architectures that force particular outputs whenever possible. AMN is *not* forced to output correspondences that satisfy the constraints of SMT; instead, conformance with SMT is reinforced through performance on training data. Our architecture uses Transformers [34] and pointer networks [35] and takes inspiration from the work of [36]. A high-level

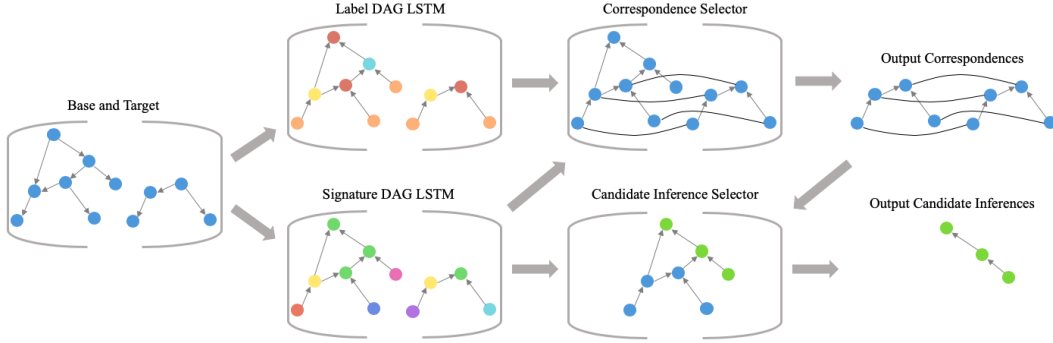


Figure 2: An overview of the model pipeline

overview is given in Figure 2, which shows how each of the three main components (graph embedding, correspondence selection, and candidate inference selection) interact with one another.

**Representing Structure:** When embedding the nodes of  $G_B$  and  $G_T$ , there are representational concerns to keep in mind. First, because matching should be done on the basis of structure, the labels of entities should not be taken into account during the alignment process. Second, because SMT’s constraints require AMN to be able to recognize when a particular node is part of multiple correspondences, AMN should maintain distinguishable representations for distinct nodes, even if those nodes have the same labels. Last, the architecture should not be vocabulary dependent, i.e., AMN should generalize to symbols it has never seen before. To achieve each of these, AMN first parses the original input into two separate graphs, a *label graph* and a *signature graph* (see Figure 3).

The label graph will be used to get an estimate of structural similarities. To generate the label graph, AMN substitutes each entity node’s label with a generic entity token. This reflects that entity labels have no inherent utility for producing matchings. Then, each function and predicate node is assigned a randomly chosen generic label (from a fixed set of such labels) based off its arity and orderedness. Assignments are made consistently across the entire graph, e.g., *every* instance of MASS in *both* the base and target would be assigned the same generic replacement label. This substitution means the original label is not used in the matching process, which allows AMN to generalize to new symbols.

The label graph is not sufficient to produce representations that can be used for the matching process, as it represents a node by only label-based features which are shared amongst different nodes (e.g., the label graph can’t distinguish between identical relations with different entities as the leaves), an issue known as the *type-token distinction* [37, 38]. To contend with this, a signature graph is constructed that represents nodes in a way that respects object identity. To construct the signature graph, AMN replaces each distinct entity with a unique identifier (drawn from a fixed set of possible identifiers). It then assigns each function and predicate a new label based solely on its arity and orderedness, ignoring the original symbol. For instance, ATTRACTS and REVOLVES-AROUND would be assigned the same label because they are both ordered predicates with arity 2.

As all input graphs will be DAGs, AMN uses two separate DAG LSTMs [39] to embed the nodes of the label and signature graphs (equations detailed in Appendix 7.2.1). Each node embedding is computed as a function of its complete set of dependencies in the original graph. The set of label structure embeddings is written as  $L_V = \{l_v : v \in V\}$  and the set of signature embeddings is written as  $S_V = \{s_v : v \in V\}$ . Before passing these embeddings to the next step, each element of  $S_V$  is scaled to unit length, i.e. each  $s_v$  becomes  $s_v / \|s_v\|$ , which gives our network an efficiently

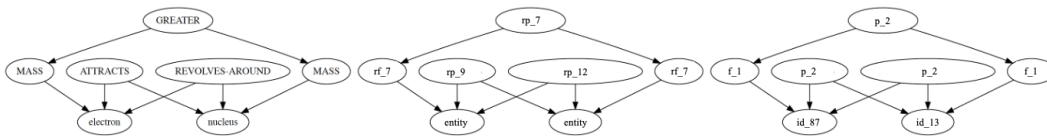


Figure 3: Original graph (left), its label graph (middle), and its signature graph (right)

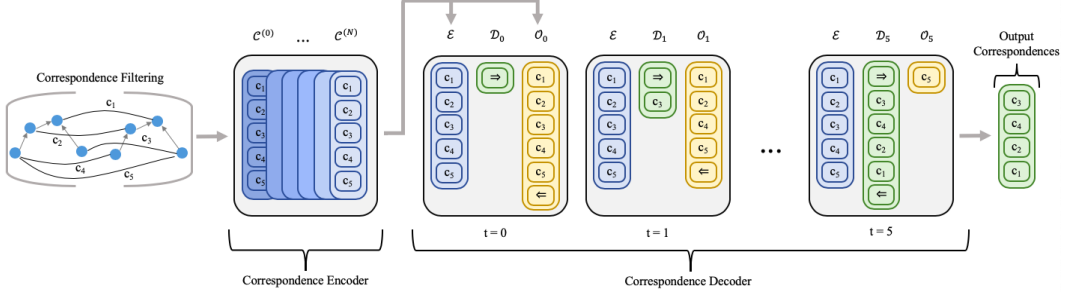


Figure 4: The correspondence selection process, where  $\Rightarrow$  and  $\Leftarrow$  are the start and stop tokens and  $\mathcal{E}$ ,  $\mathcal{D}_t$ , and  $\mathcal{O}_t$  are the sets of encoded, selected, and remaining correspondences

checkable criterion for whether or not two nodes are likely to be equal, i.e., when the dot product of two signature embeddings is 1.

**Correspondence Selector:** The graph embedding procedure yields two sets of node embeddings (label structure and signature embeddings) for the base and target. We utilize the set of embedding pairs for each node of  $V_B$  and  $V_T$ , writing  $l_v$  to denote the label structure embedding of node  $v$  taken from  $L_V$  and  $s_v$  the signature embedding of node  $v$  taken from  $S_V$ . We first define the set of unprocessed correspondences  $\mathcal{C}^{(0)}$

$$\mathcal{C}^{(0)} = \{ \langle [l_b; l_t; s_b; s_t], s_b, s_t \rangle : \langle b, t \rangle \in V_B \times V_T, \|l_b - l_t\| \leq \epsilon \}$$

where  $[\cdot; \cdot]$  denotes vector concatenation,  $\epsilon$  is the tiered identity threshold that governs how much the subgraphs rooted at two nodes may differ and still be considered for correspondence (in this work, we set  $\epsilon = 1e-5$ ). The first element of each correspondence in  $\mathcal{C}^{(0)}$ , i.e.,  $h_c = [l_b; l_t; s_b; s_t]$ , is then passed through an  $N$ -layered Transformer encoder (equations detailed in Appendix 7.2.3) to produce a set of encoded correspondences  $\mathcal{E} = \{ \langle h_c^{(N)}, s_b, s_t \rangle \in \mathcal{C}^{(N)} \}$ .

The Transformer decoder selects a subset of correspondences that constitutes the best analogical match (see Figure 4). The attention-based transformations are only performed on the initial element of each tuple, i.e.,  $h_d$  in  $\langle h_d, s_b, s_t \rangle$ . We let  $\mathcal{D}_t$  be the processed set of all selected correspondences at timestep  $t$  (after the  $N$  attention layers) and  $\mathcal{O}_t$  be the set of all remaining correspondences (with  $\mathcal{D}_0 = \{\text{START-TOK}\}$  and  $\mathcal{O}_0 = \mathcal{E} \cup \{\text{END-TOK}\}$ ). The decoder generates compatibility scores  $\alpha_{od}$  between each pair of elements, i.e.,  $\langle o, d \rangle \in \mathcal{O}_t \times \mathcal{D}_t$ . These are combined with the signature embedding similarities to produce a final compatibility  $\pi_{od}$

$$\pi_{od} = \text{FFN}([\tanh(\alpha_{od}); s_{b_o}^\top s_{b_d}; s_{t_o}^\top s_{t_d}])$$

where FFN is a two layer feed-forward network with ELU activations [40]. Recall that the signature components, i.e.  $s_b$  and  $s_t$ , were scaled to unit length. Thus, we would expect closeness in the original graph to be reflected by dot-product similarity and identity to be indicated by a maximum value dot-product, i.e.  $s_{b_o}^\top s_{b_d} = 1$  or  $s_{t_o}^\top s_{t_d} = 1$ . Once each pair has been scored, AMN selects an element of  $\mathcal{O}_t$  to be added to  $\mathcal{D}_{t+1}$ . For each  $o \in \mathcal{O}_t$ , we compute its value to be

$$v_o = \text{FFN}([\max_d \pi_{od}; \min_d \pi_{od}; \sum_d \frac{\pi_{od}}{|\mathcal{D}_t|}])$$

where FFN is a two layer feed-forward network with ELU activations. A softmax turns these scores into probabilities and the most probable element is added to  $\mathcal{D}_{t+1}$ . The use of maximum, minimum, and average is intended to let the network capture both individual and aggregate evidence. Individual evidence is given by a pairwise interaction between two correspondences (e.g., two correspondences that together violate the one-to-one constraint). Conversely, aggregate evidence is given by the interaction of a correspondence with everything selected thus far (e.g., a correspondence needed for several parallel connectivity constraints). When END-TOK is selected, the set of correspondences  $M$  returned is the set of node pairs from  $V_B$  and  $V_T$  associated with elements in  $\mathcal{D}$ .

**Candidate Inference Selector:** The output of the correspondence selector is a set of correspondences  $M$ . The candidate inferences associated with  $M$  are drawn from the nodes of the base graph

$V_B$  that were *not* used in  $M$ . Let  $V_{in}$  and  $V_{out}$  be the subsets of  $V_B$  that were and were not used in  $M$ , respectively. We first extract all signature embeddings for both sets, i.e.,  $\mathcal{S}_{in} = \{s_b : b \in V_{in}\}$  and  $\mathcal{S}_{out} = \{s_b : b \in V_{out}\}$ . In this module there are no Transformer components, with AMN operating directly on  $\mathcal{S}_{in}$  and  $\mathcal{S}_{out}$ .

AMN will select elements from  $\mathcal{S}_{out}$  to return. Like before, we let  $\mathcal{D}_t$  be the set of all selected elements from  $\mathcal{S}_{out}$  and  $\mathcal{O}_t$  be the set of all remaining elements from  $\mathcal{S}_{out}$  at timestep  $t$ . AMN computes compatibility scores between pairs of output options with candidate inference and previously selected nodes, i.e.  $\alpha_{od}$  for each  $\langle o, d \rangle \in \mathcal{O}_t \times (\mathcal{D}_t \cup \mathcal{S}_{in})$ . The compatibility scores are given by a simple single-headed attention computation (see Appendix 7.2.2). Unlike the correspondence encoder-decoder, there are no other values to combine these scores with, so they are used directly to compute a value  $v_o$  for each element of  $\mathcal{O}_t$ . AMN computes the value for a node  $o$  as

$$v_o = \text{FFN}\left(\left[\max_d \tanh(\alpha_{od}); \min_d \tanh(\alpha_{od}); \sum_d \frac{\tanh(\alpha_{od})}{|\mathcal{D}_t|}\right]\right)$$

A softmax is used and the most probable element is added to  $\mathcal{D}_{t+1}$ . Once the special end token is selected, the decoding procedure stops and returns the set of nodes associated with elements in  $\mathcal{D}$ .

## 4.2 Model Scoring

**Structural Match Scoring:** In order to avoid counting erroneous correspondence predictions towards the score of the output correspondences  $M$ , we first identify all correspondences that are either degenerate or violate the constraints of SMT. Degenerate correspondences are correspondences between constants that have no higher-order structural support in  $M$  (i.e., if either has no parent that participates in a correspondence in  $M$ ). To determine if a correspondence  $\langle b, t \rangle$  violates SMT, we check whether the subgraphs of the base and target rooted at  $b$  and  $t$  satisfy the one-to-one matching, parallel connectivity, and tiered identity constraints (see Section 3). The check can be computed in time linear with the size of the corresponding subgraphs. Let the valid subset of  $M$  be  $M_{val}$ . A correspondence  $m$  is considered a *root correspondence* if there does not exist another correspondence  $m'$  such that  $m' \in M_{val}$  and a node in  $m'$  is an ancestor of a node in  $m$ . We define  $M_{root} \subseteq M_{val}$  to be the set of all such root correspondences. For a correspondence  $m = \langle b, t \rangle$  in  $M_{val}$ , its score  $s(m)$  is given as the size of the subgraph rooted at  $b$  in the base. The structural match score for  $M$  is then sum of scores for all correspondences in  $M_{root}$ , i.e.,  $s(M) = \sum_{m \in M_{root}} s(m)$ . This repeatedly counts nodes that appear in the dependencies of multiple correspondences, which leads to higher scores for more interconnected matchings (in keeping with the systematicity preference of SMT).

**Structural Evaluation Maximization:** Dynamically assigning labels to each example allows AMN to handle never-before-seen symbols, but its inherent randomness can lead to significant variability in terms of outputs. AMN combats this by running each test problem  $r$  times and returning the predicted match  $M$  that maximizes the structural evaluation score, i.e.,  $M = \arg \max_{M_r} s(M_r)$ . Notably, AMN does not attempt to alter or correct the mapping it chooses this way, so unlike systems like SME, the mapping it returns can include constraint violations.

## 5 Experiments

### 5.1 Data Generation and Training

AMN was trained on 100,000 synthetic analogy examples, where a single example consisted of base and target graphs, a set of correspondences, and a set of nodes from the base to be candidate inferences. To generate a synthetic example, we first generated a set of random graphs  $C$ , which formed the basis for the correspondences. Next, we constructed the base  $B$  by further generating graphs around  $C$ . Likewise, for the target  $T$  we built another set of graphs around  $C$ . The graphs of  $C$  were then used to form the correspondences between the base and target. Any element in  $B$  that was an ancestor of a node from  $C$  or a descendent of such an ancestor was considered a candidate inference. Figure 5 provides an example. In the figure, the dark green nodes indicate the initial random graphs  $C$  after being copied into the base and target. The red and blue nodes show the graphs built around  $B$  and  $T$ . The light green edges indicate the gold set of correspondences generated from  $C$ . During training, each generated example was turned into a batch of inputs by repeatedly running the encoding procedure (which dynamically assigns node labels) over the original base and target.

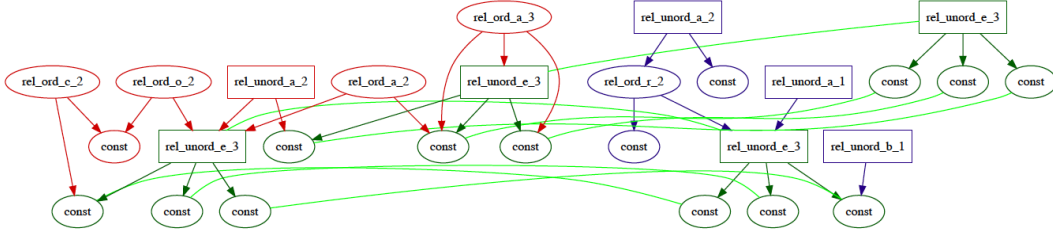


Figure 5: Synthetic example with a base (red), target (blue), and shared subgraphs (green)

## 5.2 Experimental Domains

Though all training was done with synthetic data, we evaluated the effectiveness of AMN on both synthetic data and data used in previous analogy experiments. The corpus of previous analogy examples was taken from the public release of SME<sup>1</sup>. Importantly, AMN was *not* trained on the corpus of existing analogy examples (AMN never learned from a real-world analogy example). In fact, there was *no* overlap between the symbols used in that corpus and the symbols used for the synthetic data. We briefly describe each of the domains AMN was evaluated on below (more detailed descriptions can be found in [13]). Examples of AMN’s outputs can be found in Appendix 7.3.

1. *Synthetic*: this domain consisted of 1000 examples generated with the same parameters as the training data (useful as a sanity check for AMN’s performance).
2. *Visual Oddity*: this problem setting was initially proposed to explore cultural differences to geometric reasoning in [41]. The work of [42] modeled the findings of the original experiment computationally with qualitative visual representations and analogy. We extracted 3405 analogical comparisons from the computational experiment.
3. *Moral Decision Making*: this domain was taken from the work of [43], who introduced a computational model of moral decision making that used SME to reason through moral dilemmas. From the works of [43, 44], we extracted 420 analogical comparisons.
4. *Geometric Analogies*: this domain originated from one of the first computational analogy experiments [45]. Each problem was an incomplete analogy of the form  $A : B :: C : ?$ , where each of  $A$ ,  $B$ , and  $C$  were manually encoded geometric figures and the goal was to select the figure that best completed the analogy from an encoded set of possible answers. While in the original work all figures had to be manually encoded, in [46, 47] it was shown that the analogy problems could be solved with structure-mapping over automatic encodings (produced by the CogSketch system [48]). From that work we extracted 866 analogies.

## 5.3 Results and Discussion

Table 1a shows the results for AMN across different values of  $r$ , where  $r$  denotes the re-run hyperparameter detailed in Section 4.2. When evaluating on the synthetic data, the comparison set of correspondences was given by the data generator; whereas when evaluating on the three other analogy domains, the comparison set of correspondences was given by the output of SME. It is important to note that we are using SME as our stand-in for SMT (as it is the most widely accepted computational model of SMT). Thus, we do *not* want significantly different results from SME in the correspondence selection experiments (e.g., substantially higher or lower structural evaluation scores).

In the Struct. Perf. column, the numbers reflect the average across examples of the structural evaluation score of AMN divided by that of the comparison correspondence sets. For the other columns of Table 1a, the numbers represent average fractions of examples or correspondences (e.g., 0.684 should be interpreted as 68.4%). Candidate inference prediction performance was measured relative to the set of correspondences AMN generated, i.e., all candidate inferences were computed from the *predicted* correspondences, and treated as the true positives. In many problems from the non-synthetic domains, every non-correspondence node was a candidate inference (which can lead to inflated precision and recall values). Thus, we also report the specificity (i.e., true negative rate) of AMN for *only* problems with non-candidate inference nodes.

<sup>1</sup><http://www.qrg.northwestern.edu/software/sme4/index.html>

Table 1: AMN experimental results

(a) AMN correspondence prediction results in terms of performance ratio (left), solution type rate (middle,  $\uparrow$  better), and error rate (right,  $\downarrow$  better)

Domain	$r$	Struct. Perf.	Larger	Equiv.	Err. Free	1-to-1 Err.	PC Err.	Degen. Err.
Synthetic	1	0.702	0.000	0.308	0.342	0.007	0.106	0.018
Synthetic	16	0.948	0.001	0.671	0.684	0.006	0.021	0.009
Oddity	1	0.775	0.062	0.404	0.483	0.152	0.223	0.000
Oddity	16	0.957	0.075	0.492	0.571	0.130	0.139	0.000
Moral DM	1	0.617	0.014	0.017	0.076	0.001	0.169	0.030
Moral DM	16	0.968	0.081	0.210	0.352	0.000	0.039	0.015
Geometric	1	0.870	0.066	0.539	0.654	0.041	0.116	0.000
Geometric	16	1.038	0.069	0.707	0.783	0.029	0.043	0.000

(b) AMN candidate inference prediction results

Domain	$r$	Avg. CI F1	Avg. CI Prec.	Avg. CI Rec.	Avg. CI Acc.	Avg. CI Spec.
Synthetic	16	0.899	0.867	0.964	0.860	0.733
Oddity	16	0.991	0.995	0.993	0.991	0.811
Moral DM	16	0.897	0.832	0.984	0.830	0.441
Geometric	16	0.960	0.954	0.993	0.951	0.838

**Analysis:** The left side of Table 1a shows the average ratio of AMN’s performance (labeled Struct. Perf.), as measured by structural evaluation score, against the comparison method’s performance (i.e., data generator correspondences or SME). As can be seen, AMN was around 95-104% of SME’s performance in terms of structural evaluation score on the non-synthetic domains, which indicates that it was finding similar structural matches. Again, we note that higher structural evaluation scores do *not* necessarily indicate a “better” match, as our goal is to conform to SMT’s predictions.

The middle of Table 1a gives us the best sense of how well AMN modeled SMT. We observe AMN’s performance in terms of the proportion of *larger*, *equivalent*, and *error-free* matches it produces (labeled Larger, Equiv., and Err. Free, respectively). Error-free matches do not contain degenerate correspondences or SMT constraint violations, whereas equivalent and larger matches are both error-free and have the same / larger structural evaluation score as compared to gold set of correspondences. The Equiv. column provides the best indication that AMN could model SMT. It shows that  $\approx 50\%$  of AMN’s outputs were SMT-satisfying, error-free analogical matches with the *exact same* structural score as SME (the lead computational model of SMT) in two of the non-synthetic analogy domains.

The right side of Table 1a shows the frequency of the different types of errors, including violations of the one-to-one / parallel connectivity constraints, and degenerate correspondences (labeled 1-to-1 Err., PC Err., and Degen. Err.). It shows that AMN had fairly low error rates across domains (except for Visual Oddity). Importantly, degenerate correspondences were very infrequent, which is significant because it verifies that AMN leveraged higher-order relational structure when generating matches.

Table 1b shows that AMN was fairly effective in predicting candidate inferences. The high accuracy (labeled Avg. CI Acc.) scores for both the Visual Oddity and Geometric Analogies domains indicate that AMN was able to capture the notion of structural support when determining candidate inferences. The non-zero specificity (labeled Avg. CI Spec.) results show that, while it more often classified nodes as candidate inferences, it was capable of distinguishing non-candidate inference nodes as well.

## 6 Conclusions

In this paper, we introduced the Analogical Matching Network, a neural approach that learned to produce analogies consistent with Structure-Mapping Theory. Despite being trained on completely synthetic data, AMN was capable of performing well on a varied set of analogies drawn from previous work involving analogical reasoning. AMN demonstrated renaming invariance, structural sensitivity, and the ability to find solutions in a combinatorial search space, all of which are key properties of symbolic reasoners and are known to be important to human reasoning.

## References

- [1] Dedre Gentner. Why we're so smart. *Language in mind: Advances in the study of language and thought*, 195235, 2003.
- [2] Douglas R Hofstadter. Analogy as the core of cognition. *The analogical mind: Perspectives from cognitive science*, pages 499–538, 2001.
- [3] Douglas Hofstadter. *Fluid concepts and creative analogies: Computer models of the fundamental mechanisms of thought*. Basic books, 1995.
- [4] Eyal Sagi, Dedre Gentner, and Andrew Lovett. What difference reveals about similarity. *Cognitive science*, 36(6):1019–1050, 2012.
- [5] Dedre Gentner, Sarah Brem, Ronald W Ferguson, Arthur B Markman, Bjorn B Levidow, Phillip Wolff, and Kenneth D Forbus. Analogical reasoning and conceptual change: A case study of johannes kepler. *The journal of the learning sciences*, 6(1):3–40, 1997.
- [6] Keith J Holyoak, Ellen N Junn, and Dorrit O Billman. Development of analogical problem-solving skill. *Child development*, pages 2042–2055, 1984.
- [7] Laura R Novick. Analogical transfer, problem similarity, and expertise. *Journal of Experimental Psychology: Learning, memory, and cognition*, 14(3):510, 1988.
- [8] Mary L Gick and Keith J Holyoak. Schema induction and analogical transfer. 1983.
- [9] Melanie Mitchell. *Analogy-making as perception: A computer model*. 1993.
- [10] David J Chalmers, Robert M French, and Douglas R Hofstadter. High-level perception, representation, and analogy: A critique of artificial intelligence methodology. *Journal of Experimental & Theoretical Artificial Intelligence*, 4(3):185–211, 1992.
- [11] Dedre Gentner. Structure-mapping: A theoretical framework for analogy. *Cognitive science*, 7(2):155–170, 1983.
- [12] Keith J Holyoak, Keith James Holyoak, and Paul Thagard. *Mental leaps: Analogy in creative thought*. 1996.
- [13] Kenneth D Forbus, Ronald W Ferguson, Andrew Lovett, and Dedre Gentner. Extending sme to handle large-scale cognitive modeling. *Cognitive Science*, 41(5):1152–1201, 2017.
- [14] Keith J Holyoak and Paul Thagard. Analogical mapping by constraint satisfaction. *Cognitive science*, 13(3):295–355, 1989.
- [15] Tony Veale, Diarmuid O'Donoghue, and Mark Keane. Computability as a limiting cognitive constraint: Complexity concerns in metaphor comprehension about which cognitive linguists should be aware. In *Cultural, Psychological and Typological Issues in Cognitive Linguistics: Selected papers of the bi-annual ICLA meeting in Albuquerque, July 1995*, volume 152, page 129. John Benjamins Publishing, 1999.
- [16] Tony Veale and Mark T Keane. The competence of sub-optimal theories of structure mapping on hard analogies. In *IJCAI (1)*, pages 232–237, 1997.
- [17] Danilo Ribeiro, Thomas Hinrichs, Maxwell Crouse, Kenneth Forbus, Maria Chang, and Michael Witbrock. Predicting state changes in procedural text using analogical question answering. 2013.
- [18] Maxwell Crouse, Clifton McFate, and Kenneth Forbus. Learning from unannotated qa pairs to analogically disambiguate and answer questions. In *Thirty-Second AAAI Conference on Artificial Intelligence*, 2018.
- [19] Kezhen Chen, Irina Rabkina, Matthew D McLure, and Kenneth D Forbus. Human-like sketch object recognition via analogical learning. In *Proceedings of the AAAI Conference on Artificial Intelligence*, volume 33, pages 1336–1343, 2019.
- [20] Kezhen Chen and Kenneth Forbus. Action recognition from skeleton data via analogical generalization over qualitative representations. In *Thirty-Second AAAI Conference on Artificial Intelligence*, 2018.
- [21] Matthew Klenk, Kenneth D Forbus, Emmett Tomai, Hyeonkyeong Kim, and Brian Kyckelhahn. Solving everyday physical reasoning problems by analogy using sketches. In *AAAI Conference on Artificial Intelligence*, 2005.

- [22] Scott Friedman and Kenneth Forbus. An integrated systems approach to explanation-based conceptual change. In *Twenty-Fourth AAAI Conference on Artificial Intelligence*, 2010.
- [23] Dedre Gentner and Arthur B Markman. Analogy–watershed or waterloo? structural alignment and the development of connectionist models of analogy. In *Advances in neural information processing systems*, pages 855–862, 1993.
- [24] Graeme S Halford, William H Wilson, Jian Guo, Ross W Gayler, Janet Wiles, and JEM Stewart. Connectionist implications for processing capacity limitations in analogies.
- [25] Chris Eliasmith and Paul Thagard. Integrating structure and meaning: A distributed model of analogical mapping. *Cognitive Science*, 25(2):245–286, 2001.
- [26] John E Hummel and Keith J Holyoak. Distributed representations of structure: A theory of analogical access and mapping. *Psychological review*, 104(3):427, 1997.
- [27] John E Hummel and Keith J Holyoak. Relational reasoning in a neurally plausible cognitive architecture: An overview of the lisa project. *Current Directions in Psychological Science*, 14(3):153–157, 2005.
- [28] Felix Hill, Adam Santoro, David GT Barrett, Ari S Morcos, and Timothy Lillicrap. Learning to make analogies by contrasting abstract relational structure. *International Conference on Learning Representations*, 2019.
- [29] Chi Zhang, Feng Gao, Baoxiong Jia, Yixin Zhu, and Song-Chun Zhu. Raven: A dataset for relational and analogical visual reasoning. In *Proceedings of the IEEE Conference on Computer Vision and Pattern Recognition*, pages 5317–5327, 2019.
- [30] Tomáš Mikolov, Wen-tau Yih, and Geoffrey Zweig. Linguistic regularities in continuous space word representations. In *Proceedings of the 2013 conference of the north american chapter of the association for computational linguistics: Human language technologies*, pages 746–751, 2013.
- [31] Scott E Reed, Yi Zhang, Yuting Zhang, and Honglak Lee. Deep visual analogy-making. In *Advances in neural information processing systems*, pages 1252–1260, 2015.
- [32] Brian F Bowdle and Dedre Gentner. Informativity and asymmetry in comparisons. *Cognitive Psychology*, 34(3):244–286, 1997.
- [33] Dedre Gentner and Arthur B Markman. Analogy-based reasoning. In *The handbook of brain theory and neural networks*, pages 91–93. MIT Press, 1998.
- [34] Ashish Vaswani, Noam Shazeer, Niki Parmar, Jakob Uszkoreit, Llion Jones, Aidan N Gomez, Łukasz Kaiser, and Illia Polosukhin. Attention is all you need. In *Advances in neural information processing systems*, pages 5998–6008, 2017.
- [35] Oriol Vinyals, Meire Fortunato, and Navdeep Jaitly. Pointer networks. In *Advances in neural information processing systems*, pages 2692–2700, 2015.
- [36] Wouter Kool, Herke Van Hoof, and Max Welling. Attention, learn to solve routing problems! *arXiv preprint arXiv:1803.08475*, 2018.
- [37] Daniel Kahneman, Anne Treisman, and Brian J Gibbs. The reviewing of object files: Object-specific integration of information. *Cognitive psychology*, 24(2):175–219, 1992.
- [38] Linda Wetzel. Types and tokens. 2006.
- [39] Maxwell Crouse, Ibrahim Abdelaziz, Cristina Cornelio, Veronika Thost, Lingfei Wu, Kenneth Forbus, and Achille Fokoue. Improving graph neural network representations of logical formulae with subgraph pooling. *arXiv preprint arXiv:1911.06904*, 2019.
- [40] Djork-Arné Clevert, Thomas Unterthiner, and Sepp Hochreiter. Fast and accurate deep network learning by exponential linear units (elus). *arXiv preprint arXiv:1511.07289*, 2015.
- [41] Stanislas Dehaene, Véronique Izard, Pierre Pica, and Elizabeth Spelke. Core knowledge of geometry in an amazonian indigene group. *Science*, 311(5759):381–384, 2006.
- [42] Andrew Lovett and Kenneth Forbus. Cultural commonalities and differences in spatial problem-solving: A computational analysis. *Cognition*, 121(2):281–287, 2011.
- [43] Morteza Dehghani, Emmett Tomai, Ken Forbus, Rumien Iliev, and Matthew Klenk. Moraldm: A computational modal of moral decision-making. In *Proceedings of the Annual Meeting of the Cognitive Science Society*, 2008.

- [44] Morteza Dehghani, Emmett Tomai, Kenneth D Forbus, and Matthew Klenk. An integrated reasoning approach to moral decision-making. In *AAAI*, pages 1280–1286, 2008.
- [45] Thomas G Evans. A program for the solution of a class of geometric-analogy intelligence-test questions. Technical report, AIR FORCE CAMBRIDGE RESEARCH LABS LG HANSCOM FIELD MASS, 1964.
- [46] Andrew Lovett, Emmett Tomai, Kenneth Forbus, and Jeffrey Usher. Solving geometric analogy problems through two-stage analogical mapping. *Cognitive science*, 33(7):1192–1231, 2009.
- [47] Andrew Lovett and Kenneth Forbus. Modeling multiple strategies for solving geometric analogy problems. In *Proceedings of the Annual Meeting of the Cognitive Science Society*, volume 34, 2012.
- [48] Kenneth Forbus, Jeffrey Usher, Andrew Lovett, Kate Lockwood, and Jon Wetzel. Cogsketch: Sketch understanding for cognitive science research and for education. *Topics in Cognitive Science*, 3(4):648–666, 2011.
- [49] Adam Paszke, Sam Gross, Francisco Massa, Adam Lerer, James Bradbury, Gregory Chanan, Trevor Killeen, Zeming Lin, Natalia Gimelshein, Luca Antiga, et al. Pytorch: An imperative style, high-performance deep learning library. In *Advances in Neural Information Processing Systems*, pages 8024–8035, 2019.
- [50] Diederik P Kingma and Jimmy Ba. Adam: A method for stochastic optimization. *arXiv preprint arXiv:1412.6980*, 2014.
- [51] Kai Sheng Tai, Richard Socher, and Christopher D Manning. Improved semantic representations from tree-structured long short-term memory networks. In *Proceedings of the 53rd Annual Meeting of the Association for Computational Linguistics and the 7th International Joint Conference on Natural Language Processing (Volume 1: Long Papers)*, pages 1556–1566, 2015.
- [52] Jimmy Lei Ba, Jamie Ryan Kiros, and Geoffrey E Hinton. Layer normalization. *arXiv preprint arXiv:1607.06450*, 2016.

## 7 Appendix

### 7.1 Model Details

In the DAG LSTM, the node embeddings were 32-dimensional vectors and the edge embeddings were 16-dimensional vectors. For all Transformer components, our model used multi-headed attention with 2 attention layers each having 4 heads. In each multi-headed attention layer, the query and key vectors were projected to 128-dimensional vectors. The feed forward networks used in the Transformer components had one hidden layer with a dimensionality twice that of the input vector size. The feed forward networks used to compute the values in the correspondence selector used two 64-dimensional hidden layers. The models were constructed with the Pytorch [49] library.

**Loss Function:** As both the correspondence and candidate inference components use a softmax, the loss function is categorical cross entropy. Teacher forcing is used to guide the decoder to select the correct choices during training. With  $\mathcal{L}_{corr}$  the loss for correspondence selection and  $\mathcal{L}_{ci}$  the loss for candidate inference selection, the final loss is given as  $\mathcal{L} = \mathcal{L}_{corr} + \lambda\mathcal{L}_{ci}$  (with  $\lambda = 0.1$  in our experiments), which is minimized with Adam [50].

### 7.2 Background

#### 7.2.1 DAG LSTMs

DAG LSTMs extend Tree LSTMs [51] to DAG-structured data. As with Tree LSTMs, DAG LSTMs compute each node embedding as the aggregated information of all their immediate predecessors (the equations for the DAG LSTM are identical to those of the Tree LSTM). The difference between the two is that DAG LSTMs stage the computation of a node’s embedding based on the order given by a topological sort of the input graph. Batching of computations is done by grouping together updates of independent nodes (where two nodes are independent if they are neither ancestors nor predecessors

of one another). As in [39], for a node,  $v$ , its initial node embedding,  $s_v$ , is assigned based on its label and arity. The DAG LSTM then computes the final embedding  $h_v$  to be

$$\begin{aligned}
i_v &= \sigma(W_i s_v + \sum_{w \in \mathcal{P}(v)} U_i^{(e_{vw})} h_w + b_i) \\
o_v &= \sigma(W_o s_v + \sum_{w \in \mathcal{P}(v)} U_o^{(e_{vw})} h_w + b_o) \\
\hat{c}_v &= \tanh(W_c s_v + \sum_{w \in \mathcal{P}(v)} U_c^{(e_{vw})} h_w + b_c) \\
f_{vw} &= \sigma(W_f s_v + U_f^{(e_{vw})} h_w + b_f) \\
c_v &= i_v \odot \hat{c}_v + \sum_{w \in \mathcal{P}(v)} f_{vw} \odot c_w \\
h_v &= o_v \odot \tanh(c_v)
\end{aligned}$$

where  $\odot$  is element-wise multiplication,  $\sigma$  is the sigmoid function,  $\mathcal{P}$  is the predecessor function that returns the arguments for a node,  $U_i^{(e_{vw})}$ ,  $U_o^{(e_{vw})}$ ,  $U_c^{(e_{vw})}$ , and  $U_f^{(e_{vw})}$  are learned matrices per edge type.  $i$  and  $o$  represent input and output gates,  $c$  and  $\hat{c}$  are memory cells, and  $f$  is a forget gate.

## 7.2.2 Multi-Headed Attention

The multi-headed attention (MHA) mechanism of [34] is used in our work to compare correspondences against one another. In this work, MHA is given two inputs, a query vector  $q$  and a list of key vectors to compare the query vector against  $\langle k_1, \dots, k_n \rangle$ . In  $N$ -headed attention,  $N$  separate attention transformations are computed. For transformation  $i$  we have

$$\begin{aligned}
\hat{q}_i &= W_i^{(q)} q, k_{ij} = W_i^{(k)} k_j, v_{ij} = W_i^{(v)} k_j \\
w_{ij} &= \frac{\hat{q}_i^\top k_{ij}}{\sqrt{b_{\hat{q}}}} \\
\alpha_{ij} &= \frac{\exp(w_{ij})}{\sum_{j'} \exp(w_{ij'})} \\
q_i &= \sum_j \alpha_{ij} \hat{q}_i
\end{aligned}$$

where each of  $W_i^{(q)}$ ,  $W_i^{(k)}$ , and  $W_i^{(v)}$  are learned matrices and  $b_{\hat{q}}$  is the dimensionality of  $\hat{q}_i$ . The final output vector  $q'$  for input  $q$  is then given as a combination of its  $N$  transformations

$$q' = \sum_{i=1}^N W_i^{(o)} q_i$$

where each  $W_i^{(o)}$  is a distinct learned matrix for each  $i$ . In implementation, the comparisons of query and key vectors are batched together and performed as efficient matrix multiplications.

## 7.2.3 Transformer Encoder-Decoder

The Transformer-based encoder-decoder is given two inputs, a comparison set  $\mathcal{C}$  and an output set  $\mathcal{O}$ . At a high level,  $\mathcal{C}$  will be encoded into a new set  $\mathcal{E}$ , which will inform a selection process that picks elements of  $\mathcal{O}$  to return. In the context of pointer networks, the set  $\mathcal{O}$  begins as the encoded input set (i.e.,  $\mathcal{O} \equiv \mathcal{E}$ ).

**Encoder:** First, the elements of  $\mathcal{C}$ , i.e.  $h_c \in \mathcal{C}$ , are passed through  $N$  layers of an attention-based transformation. For element  $h_c$  in the  $i$ -th layer (i.e.,  $h_c^{(i-1)}$ ) this is performed as follows

$$\begin{aligned}
\hat{h}_c &= \text{LN}(h_c^{(i-1)} + \text{MHA}_{\mathcal{C}}^{(i)}(h_c^{(i-1)}, \langle h_1^{(i-1)}, \dots, h_j^{(i-1)} \rangle)) \\
h_c^{(i)} &= \text{LN}(\hat{h}_c + \text{FFN}^{(i)}(\hat{h}_c))
\end{aligned}$$



